Journal of Marine Research, 51, 237–271, 1993

Journal of
MARINE RESEARCH

Volume 51, Number 2

On the role of large bubbles in air-sea gas exchange and supersaturation in the ocean

by Ralph F. Keeling[1,2]

ABSTRACT

A parameterization of bubble-induced gas exchange is presented in which the bubble contribution to gas exchange is expressed in terms of separate transfer velocities for ingassing (K_b^{in}) and outgassing (K_b^{out}). The difference between the ingassing and outgassing velocities ($K_b^{in} - K_b^{out}$) is further separated into two components, the first caused by the injection of small bubbles into the water, the second caused by gas exchange across the surface of hydrostatically compressed larger bubbles. It is argued that both K_b^{out} and the exchange contribution to the difference $K_b^{in} - K_b^{out}$ should be largely independent of the dissolved concentrations of the major gases N_2 and O_2.

A simple model is presented which allows K_b^{out} and the exchange contribution to the difference $K_b^{in} - K_b^{out}$ to be estimated. The model incorporates data from laboratory simulation experiments on the bubble production spectrum. The results indicate that bubbles larger than 0.05 cm in radius, which have often been assumed to play a negligible role, contribute significantly to bubble-induced gas exchange and supersaturation in the ocean. The model is used to explore the sensitivity of bubble-induced gas exchange to the overall air entrainment rate, size and depth distributions of the bubbles, and to the gas exchange rates across the surface of individual bubbles.

The model suggests that bubbles may make an important contribution to overall gas exchange at windspeeds above 10 m sec^{-1}. In this regime gas transfer velocities should depend, not just on diffusivity, but also on the solubility of the gases. It is suggested that $K_b^{(out)}$ should scale roughly as $\alpha^{-0.3}D^{0.35}$ where α is the solubility and D is the diffusivity. The model results, in combination with measurements on inert gas supersaturations, suggest that the global-mean

1. National Center for Atmospheric Research, 1850 Table Mesa Road, Boulder, Colorado, 80307-3000, U.S.A.

Present address: Scripps Institution of Oceanography, 9500 Gilman Dr., Dept. 0236, La Jolla, California, 92093-0236, U.S.A.

supersaturation of CO_2 induced by bubbles is not larger than 0.3% and most probably is around 0.08%. A major uncertainty results from a lack of information on production rates and distributions of large bubbles. Several possible experiments are proposed for improving estimates of bubble-induced gas exchange and supersaturation.

1. Introduction

Bubbles produced at the ocean surface as the result of breaking waves represent a potentially important pathway for transporting gases between the ocean and the atmosphere. Although bubbles have been shown to contribute only a fraction of gas exchange measured in experiments with wind/wave tunnels (see e.g. Broecker and Siems, 1984), the fetches used in these experiments are too short to accurately simulate the appropriate levels of turbulence and rates of bubble production (see e.g. Thorpe, 1984). As yet, there are no direct measurements of the contribution of bubbles to gas exchange in the open ocean. The role of bubbles in air-sea gas exchange remains poorly understood.

If bubbles contribute significantly to overall gas exchange in the open ocean, this would invalidate several assumption upon which air-sea exchange rates are typically calculated. For example, it is commonly assumed that the exchange rates can be parameterized according to a transfer or piston velocity K which is independent of the solubility of the gas but increases according to the one-half or two-thirds power of the diffusivity of the gas in water (e.g. Liss and Merlivat, 1986). This power law has been confirmed for wind/wave tunnel experiments (Ledwell, 1984; Jähne *et al.*, 1987b) but not yet confirmed for the open ocean. If bubble-induced exchange is important, however, the transfer velocity would, in general, depend both on the diffusivity and the solubility of the gas, with smaller values for gases with higher solubilities. It has also been common practice to assume that exchange velocities in the open ocean scale roughly linearly or quadratically with wind speed in accordance with wind/wave tunnel experiments (Liss and Merlivat, 1986; Wanninkhof, 1992). If bubble exchange is important, however, the transfer velocity would be expected to increase roughly in proportion to the area covered with white caps, which increases at around the third or fourth power of the wind speed (Monahan and Muircheartaigh, 1980; Monahan, 1993).

Another assumption which becomes questionable in the presence of bubble-induced gas exchange is the notion that the exchange flux is strictly proportional to the partial-pressure difference between water and air. Unlike the exchange that takes place at the surface of the ocean, which drives the concentration of dissolved gases towards equilibrium with the atmosphere, bubble exchange drives seawater towards a slight supersaturation. The supersaturation arises because the air in the bubbles is compressed as a result of surface tension and hydrostatic pressure. Bubbles are believed to contribute to an average supersaturation of a few percent for

relatively insoluble gases such as helium and oxygen (Craig and Weiss, 1970; Craig and Hayward, 1987; Spitzer and Jenkins, 1989). Bubbles also may tend to drive more soluble gases, such as CO_2, toward a slight supersaturation, although the extent of this supersaturation is not well known.

Bubble-induced gas exchange varies qualitatively depending on the size of the bubbles. In rough terms we can consider three size regimes: (1) small bubbles ($r < 0.005$ cm) which completely disappear by dissolution in the water, (2) intermediate bubbles in which the gases equilibrate with gases dissolved in the water, and (3) large bubbles ($r > 0.05$ cm) in which the gases do not equilibrate with the water (Jähne *et al.*, 1984; Memery and Merlivat, 1985b). Although all three size classes may be important in exchange of relatively insoluble gases like He and O_2, only the large size class can contribute significantly to exchange and supersaturation of soluble gases like CO_2. This follows because gas exchange by small and intermediate sized bubbles is limited by the capacity of the bubbles to store gases when in equilibrium in the water, and this leads to exchange velocities which tend to scale inversely with the solubility of the gas. With carbon dioxide being 30 to 60 times more soluble in seawater than gases like O_2 and He, it follows that the enhancement of gas exchange and supersaturation of CO_2 by the intermediate and small bubbles must be 30 to 60 times smaller than that for insoluble gases like O_2 and He.

The exchange of gases across large bubbles is limited primarily by the kinetic barrier to transfer at the aqueous surface of the bubble rather than by the equilibrium capacity of the bubbles. Like the exchange which takes places at the air-sea interface, this leads to an exchange velocity which scales, typically, as the square-root of the diffusivity of the gas in water, but is independent of solubility. Importantly, large bubbles have the potential to enhance the air-sea exchange of CO_2 and produce supersaturations in CO_2 at the same level as for less soluble gases like He and O_2.

This paper has the following primary objectives: (1) to clarify the relationship between bubble-induced gas exchange and bubble-induced supersaturation, (2) to explore the sensitivity of bubble-induced gas exchange and supersaturation on the physicochemical properties (solubility and diffusivity) of the gas in question ranging from insoluble gases like He and O_2, to soluble gases like CO_2, and (3) to explore the role of large bubbles ($r > 0.05$ cm) on air-sea gas exchange and supersaturation. The remainder of this paper is organized as follows: Section 2 proposes a method of parameterizing bubble-induced gas exchange in terms of separate ingassing and outgassing exchange velocities. Section 3 presents a simple model for calculating these exchange velocities. Section 4 discusses estimates of the various quantities which enter the calculations of the exchange coefficients. Section 5 presents the results of the model calculations including sensitivity analyses. Section 6 discusses the implications of the model results and suggests where additional research would be useful. Section 7 summarizes the main conclusions.

2. Parameterization of gas exchange due to bubbles

The gas exchange through the sea surface is commonly parameterized according to

$$F_s = K_s S\,(P_g - P_l) \tag{1}$$

where F_s (moles cm^{-2} sec^{-1}) is the air-to-sea gas flux, S (moles cm^{-3} atm^{-1}) is the solubility of the gas, P_g (atm) is the partial pressure of the gas in the air, P_l (atm) partial pressure of the gas exerted by the water, and K_s (cm sec^{-1}) is the gas exchange or piston velocity. Eq. (1) also can be written

$$F_s = -K_s S P_g f \tag{2}$$

where f is the fractional supersaturation given by

$$f = \frac{P_l}{P_g} - 1. \tag{3}$$

An analogous expression which accounts for the gas exchange between the air and water mediated by the bubbles produced by breaking waves can be written

$$F_b = K_b^{\text{in}} S P_g - K_b^{\text{out}} S P_l \tag{4}$$

where K_b^{in} is the one-way exchange velocity for ingassing (air to sea) and K_b^{out} is the one-way exchange velocity for outgassing (sea to air). Here we need different exchange velocities for ingassing and outgassing because we are multiplying the ingassing velocity K_b^{in} by the partial pressure in the atmosphere P_g rather than the partial pressure in the bubbles themselves. Bubble pressure exceeds atmosphere pressure because of surface tension and hydrostatic compression, and thus, in general we require $K_b^{\text{in}} > K_b^{\text{out}}$.

Combining Eqs. (1) and (4) we can derive a relation for the net flux F_{tot} due to the combined effects of bubbles and surface exchange:

$$F_{\text{tot}} = F_s + F_b = (K_s + K_b^{\text{out}}) S (P_g - P_l) + (K_b^{\text{in}} - K_b^{\text{out}}) S P_g. \tag{5}$$

An important consequence of Eq. (5) is that the net flux is not zero when the water and air are in equilibrium. Instead, the flux is zero at a steady-state when the seawater is supersaturated by an amount given by

$$f_0 = \frac{K_b^{\text{in}} - K_b^{\text{out}}}{K_s + K_b^{\text{out}}}. \tag{6}$$

Using Eq. (6), we can rewrite Eq. (5) as

$$F_{\text{tot}} = -(K_b^{\text{out}} + K_s) S P_g (f - f_0). \tag{7}$$

Comparing Eqs. (7) and (2) we see that exchange with bubbles is analogous to exchange without bubbles except that the overall transfer rate coefficient is increased

by the term K_b^{out}, and the flux is now proportional to the difference between the actual supersaturation and the steady-state supersaturation given by Eq. (6).

An alternative parameterization of bubble-induced gas exchange has been proposed by Fuchs *et al.* (1987). Here we consider a modification of the Fuchs *et al.* parameterization in which the total air-sea gas flux caused by bubbles is divided into two components: The first component consists of gas which is injected into the water by bubbles which disappear by dissolution. This process, which accounts for the effects of small bubbles ($r < 0.005$ cm radius) which tend to totally disappear by dissolution (Merlivat and Memery, 1983), results in the net transfer of gas of atmospheric composition into the water. The second component includes the combined effects of the intermediate sized bubbles, which are small enough to equilibrate with the water, and large bubbles which do not equilibrate. (Fuchs *et al.* (1987) further subdivide the second component into intermediate and large fractions.)

With this second parameterization, the air-sea gas flux due to bubbles is given by

$$F_b = \frac{P_g}{RT}\left[V_{inj} + V_{exch}\left(\frac{\Delta P}{P_0} - f\right)\right] \tag{8}$$

where V_{inj} is the air-injection rate for the small bubbles, V_{exch} is a gas exchange rate for the larger bubbles, ΔP is a measure of the effective total over-pressure of the larger bubbles relative to atmospheric pressure, and P_0 is the total atmospheric pressure. Both V_{inj} and V_{exch} have units of volume of air per unit of surface per unit time, so they correspond to piston velocities expressed with respect to the air. The coefficient V_{inj}, which essentially depends on the production rate of small bubbles, is defined to be the same for all gases. The coefficient V_{exch} essentially depends on the production rates of larger bubbles and varies depending on the physicochemical properties of the gas. The ratio $\Delta P/P_0$ is closely related to the average depth of the larger bubbles because the "overpressure" on the bubbles is mostly dependent on the weight of the water above. The relationship between the coefficients V_{exch} and $\Delta P/P_0$ and the bubble production rates and depths is explored using the model presented in the next section.

The two formulations of bubble-induced gas exchange (Eq. (4) and Eq. (8)) can be related by matching the terms with factors of P_g and P_l in Eq. (8) and Eq. (4), using Eq. (3). This yields

$$K_b^{out} = \frac{V_{exch}}{\alpha} \tag{9}$$

and

$$K_b^{in} - K_b^{out} = \frac{V_{inj}}{\alpha} + \frac{\Delta P}{P_0}\frac{V_{exch}}{\alpha} \tag{10}$$

where $\alpha = SRT$ is the Ostwald solubility coefficient (IUPAC, 1979) which is dimensionless. Eq. (10) shows that the difference $K_b^{in} - K_b^{out}$ can be separated into an "air-injection" component V_{inj}/α and "exchange" component $(\Delta P/P_0)\, K_b^{out}$.

The steady-state supersaturation can similarly be separated into an "air-injection" component and an "exchange" component according to

$$f_0 = f_0^{(inj)} + f_0^{(exch)}$$

where

$$f_0^{(inj)} = \frac{V_{inj}/\alpha}{K_s + K_b^{out}} \tag{12}$$

and

$$f_0^{(exch)} = \left(\frac{\Delta P}{P_0}\right)\left(\frac{V_{exch}}{\alpha K_s + V_{exch}}\right) = \left(\frac{\Delta P}{P_0}\right)\left(\frac{K_b^{out}}{K_s + K_b^{out}}\right)$$

Eq. (13) shows $f_0^{(exch)}$ is directly proportional to the percentage of the total air-sea exchange contributed by bubbles with a proportionality factor of $\Delta P/P_0$.

Thus far we have neglected one important complication involving bubble-induced gas exchange. The dynamics of bubbles, specifically their tendency to expand or contract beneath the surface, can depend on the dissolved concentrations of the major gases O_2 and N_2 (Thorpe, 1982; Merlivat and Memery, 1983). This dependence arises because bubbles tend to loose gas by dissolution when the internal bubble pressure exceeds the total gas pressure in the water and they tend to gain gas when the opposite is true. The net tendency for bubbles to grow or contract therefore depends, in part, on the dissolved concentrations of the major gases. Likewise, the bubble-induced gas exchange coefficients must be allowed, in general, to depend on the dissolved concentration of major gases. This allowance must be made whether we are considering air-sea exchange of trace gases or air-sea exchange of the major gases, themselves. The gas exchange flux for the major gases thus is a non-linear function of their partial pressures in the water.

This parameterization (Eq. (8)) allows an important simplification to be made with regard to the dependence of gas exchange on the major gases. The simplification is that, of the three gas exchange parameters (V_{inj}, V_{exch}, and $\Delta P/P_0$), only V_{inj} depends significantly on the dissolved concentration of the major gases. This simplification is justified because, as shown in Section 5 below, V_{exch} and $\Delta P/P_0$ depend mostly on bubbles larger than 0.03 cm in radii. Bubbles larger than 0.03 cm rise to the surface on a time scale that is at least 10 times faster than the time scale for them to dissolve in the water (Jähne *et al.*, 1984). The dynamics of the bubbles which contribute to V_{exch} and $\Delta P/P_0$ are therefore largely independent of the dissolved concentrations of

Table 1. Functional dependencies of exchange parameters

Gas Exchange Parameter	Units	Functional Form*
V_{inj}	cm sec^{-1}	V_{inj} {P_{N_2}, P_{O_2}, Dyn.}
V_{exch}	cm sec^{-1}	V_{exch} {$\alpha D^{1/2}$, Dyn.}#
$\Delta P/P_0$	dimensionless	$\frac{\Delta P}{P_0}$ {$\alpha D^{1/2}$, Dyn.}#
K_b^{out}	cm sec^{-1}	$\frac{1}{\alpha} V_{exch}$
$K_b^{in} - K_b^{out}$	cm sec^{-1}	$\frac{1}{\alpha}\left(V_{inj} + \frac{\Delta P}{P_0} V_{exch}\right)$

*P_{N_2} and P_{O_2} denote dependence on the partial pressures of the major gases O_2 and N_2 in the water. Dyn. denotes dependence on bubble dynamics and thus on variables such as wind speed, atmospheric stability, wave age, surface tension, etc.

#That the functional dependence on solubility and diffusivity is embraced by the single parameter $\alpha D^{1/2}$ is shown in Section 4.

the major gases. Table 1 summarizes the different gas exchange parameters and the variables on which they are assumed to depend.

3. A model of gas exchange due to bubbles

In this section, a simple model for calculating the bubble exchange parameters V_{exch} and $\Delta P/P_0$ is presented. Because the parameter V_{inj} already accounts for the exchange caused by the smallest bubbles, which are injected, this model is aimed primarily at representing exchange caused by intermediate and large sized bubbles.

The gas exchange model is largely based on the simplified picture of bubble dynamics proposed by Merlivat and Memery (1983) and Memery and Merlivat (1985a). Bubbles are assumed to be rapidly submersed to a particular depth without any gas being exchanged. The bubbles then rise at their terminal velocity back to the surface. As the bubbles rise, gases are exchanged across the bubble surface. On average, bubble populations are assumed to decrease exponentially with depth with a characteristic depth which is allowed to depend on bubble radius. The total gas pressure in the bubble is assumed to be equal to the local hydrostatic pressure; thus the effect of surface tension on bubble pressure is neglected. Bubbles are assumed to be carried to depths of at most a few meters so that the percentage change in bubble radii due to hydrostatic compression can be treated as a small parameter.

The model presented here differs from the treatment of Memery and Merlivat (1985a) in one significant respect. As bubbles rise back to the surface they tend to expand as they undergo hydrostatic decompression, while, at the same time they tend to contract as the gas in them dissolves. Memery and Merlivat assumed that these two effects cancel, such that the bubble radius is invariant with depth. In fact, however, the relative magnitude of the two effects depends strongly on bubble radius, with the larger bubbles tending to expand as they rise, while smaller bubbles tend to contract (Thorpe, 1982; Merlivat and Memery, 1983; Jähne *et al.,* 1984).

In the model presented here, the contraction caused by dissolution is neglected and bubble radius is assumed to be governed only by hydrostatic decompression. This assumption leads to the correct radius-depth relation in the large bubble limit because dissolution becomes negligible for large bubbles. The considerations of Jähne *et al.* (1984) and Merlivat and Memery (1983) suggest that this assumption is reasonable for bubbles larger than 0.03 cm in radius. Although the assumption is clearly not valid for smaller bubbles, the calculations below are nevertheless extended over the full spectrum of bubble sizes, including bubbles smaller than 0.03 cm radius. This extension of the model can be justified as follows.

By neglecting the tendency of bubbles to contract by dissolution of the major gases, the model underestimates the partial pressure of the residual gases. The model therefore underpredicts the magnitude of the inward exchange coefficient K_b^{in}. As pointed out by Jähne *et al.* (1984), however, the time required for the total number of moles of gas in a bubble to change is considerably longer than the time required for an individual component to come into equilibrium with the water. Thus the contraction caused by dissolution of the bubble as a whole tends to inject gases into the water in proportion to their abundance in equilibrated air. Gases which are near equilibrium with the overlying atmosphere thus tend to be injected into the water in proportion to their abundance in the overlying air. We can rationalize neglecting this effect because we have approximately accounted for it through the air-injected component V_{inj} which we are not attempting to model here. Of course, with this approach, we must allow that the air injection velocity V_{inj} accounts not just for small bubbles which are fully injected, but also for somewhat larger bubbles which are partially injected. For gases which are not near equilibrium, the air injection process can generally be neglected since $|f| \gg |f_0|$ (see Eq. (7)). We can thus rationalize neglecting the tendency of bubbles to contract when estimating exchange parameters K_b^{out} and $\Delta P/P_0$ for all gases regardless of their dissolved concentrations.

A second consequence of neglecting the contraction caused by dissolution is that it leads to an overestimation of the ultimate size of the small bubbles ($r < 0.03$ cm) when they reach the surface (if they ever do). It thus leads the model to overestimate the contribution of small bubbles to the outward exchange coefficient K_b^{out}. However, subsequent calculations, which are based on this assumption, indicate that $K_b^{(out)}$ and $\Delta P/P_0$ are dominated by bubbles larger than 0.03 cm in radius. Overestimating the

contribution of bubbles smaller than 0.03 cm therefore can have little effect on the results.

The exchange of a particular gas component across the surface of an individual bubble is parameterized according to

$$\frac{dn}{dt} = k(r)r^2S(P_l - P_b)$$

where n is the number of moles of this gas in the bubble, r is the bubble radius, P_1 and P_b are the partial pressures of the gas in the liquid and in the bubble, respectively, and $k(r)$ is the gas tranfer velocity for an individual bubble. Applying Eq. (14) to the model of bubble dynamics described above allows the exchange parameters to be calculated. Details of the model are worked out in the Appendix.

The resulting exchange parameters can conveniently be expressed in terms of three length scales: (1) z_0, the characteristic (e-folding) depth of the bubble population (2) H_0, the fixed depth (approximately 10 m) at which the hydrostatic pressure is twice the atmospheric pressure, and (3) the vertical distance H_{eq} over which the bubble must rise before partial pressure differences between the bubble and the water are reduced by a factor of $1/e$. The parameter H_{eq} depends on the physicochemical properties of the gas in question; z_0 and H_0 are, of course, the same for all gases.

The following results are obtained for the exchange parameters

$$V_{exch} = \int_0^\infty \frac{4\pi}{3} r^3 Q(r)E(r)\,dr$$

$$\frac{\Delta P}{P} \cdot V_{exch} = \int_0^\infty \frac{4\pi}{3} r^3 Q(r)F(r)\,dr$$

where $Q(r)$ is the number of bubbles with radii between r and $r + dr$ entrained per unit sea-surface area per unit time. The factors $E(r)$ and $F(r)$, both dimensionless, are given by

$$E(r) = \frac{z_0(r)}{z_0(r) + H_{eq}(r)} \tag{17}$$

and

$$F(r) = \frac{H_{eq}(r)}{H_0} \frac{z_0(r)^2}{(z_0(r) + H_{eq}(r))^2}. \tag{18}$$

The equilibration distance H_{eq} is given by

$$H_{eq}(r) = \left(\frac{4\pi}{3\alpha}\right)\left(\frac{rU(r)}{k(r)}\right) \tag{19}$$

where $U(r)$ is bubble rise velocity.

Eq. (15) has a relatively simple interpretation. The gas tranfer velocity V_{exch} is simply the volume of air $4\pi/3\, r^3\, Q(r)dr$ entrained by bubbles with radii between r and $r + dr$ multiplied by a dimensionless efficiency factor $E(r)$ integrated over the bubble size distribution. This efficiency factor is proportional to the extent to which the gas in the bubbles comes into equilibrium with the water, approaching the limit 1.0 as the gas fully equilibrates ($H_{eq}/z_0 \rightarrow 0$).

To proceed, we need expressions for the bubble rise velocity $U(r)$, the gas exchange coefficient for an individual bubble $k(r)$, the characteristic depth $z_0(r)$, and the bubble source spectrum $Q(r)$. These quantities are the subject of the next section.

4. Model input parameters

a. Bubble rise velocities and gas transfer velocities. We assume that the rise velocity is equal to the terminal velocity which is calculated by equating the buoyancy force and the drag force:

$$\rho g \frac{4\pi}{3} r^3 = C_D \frac{\pi r^2}{2} \rho U^2$$

where ρ is the density, g is the gravitational acceleration and C_D is the drag coefficient.

For the drag coefficient we take $C_D = 24/(1 + 0.566\, Re^{0.5})/Re$ where $Re = 2rU/\nu$ is the Reynolds number and ν is the kinematic viscosity. This relation for the drag coefficient agrees with Stoke's Law for "dirty" (i.e. surfactant covered) bubbles in the small-bubble limit ($Re \rightarrow 0$) and overlaps with the relation of Moore (1963) for intermediate-sized bubbles ($40 < Re < 200$). For radii larger than ~ 0.056 cm, where this relationship predicts a rise velocity greater than 30 cm sec^{-1}, we employ a constant rise velocity of 30 cm sec^{-1} as per Levich (1962). This relation between terminal velocity and radius for seawater at 20°C, is shown in Figure 1.

For the gas exchange coefficient, we take the relation for "clean" bubbles given by

$$k(r) = 8\sqrt{\frac{\pi DU(r)}{2r}}$$

(see Levich (1962) Section 91, also see Memery and Merlivat (1985a)) where D is the diffusion coefficient. Since bubble drag is dominated by the small region in the trailing edge of the bubble where surfactants tend to concentrate (Levich, 1962), whereas gas exchange occurs more uniformly over the full bubble surface, it is not inconsistent to employ relations for "clean" bubbles to compute gas exchange while employing relations for "dirty" bubbles to compute rise velocities, as has been done here.

Eqs. (20) and (21) are valid only for bubbles rising through still water, so their applicability to the turbulent conditions which prevail in whitecaps is questionable.

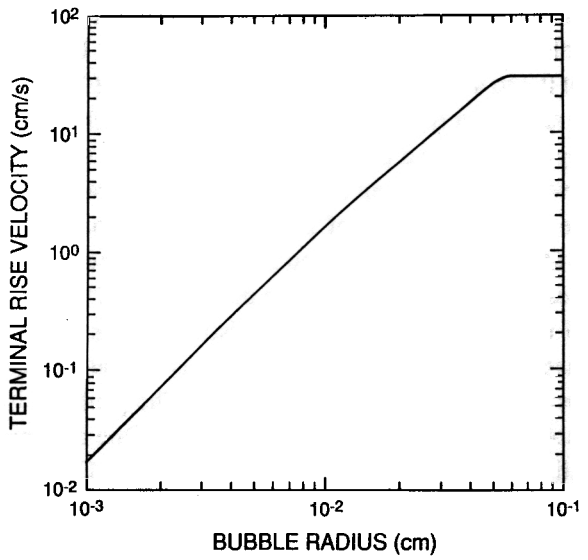

Figure 1. Terminal rise velocity versus bubble radius for "dirty" bubbles, computed using relations in text.

For example, it is to be expected that turbulence could decrease the rate at which bubbles rise through the water by increasing the drag. In fact, Broecker and Siems (1984) observed a decrease in rise velocities associated with breaking waves in a wind-wave tunnel experiment. Turbulence may also increase the gas exchange rate across the surface of bubbles relative to the rate expected in still water. To test the sensitivity of the results to these turbulence effects, calculations will be carried out in which $k(r)$ is arbitrarily increased by a factor of four relative to the value given by Eq. (21). Since $U(r)$ and $k(r)$ influence the exchange parameters through the quantity H_{eq} alone, increasing $k(r)$ by a factor of four has the same effect as decreasing $U(r)$ by a factor of four (see Eq. (19)).

One important consequence of Eq. (21) and Eq. (19) is that the full gas-dependence of H_{eq} (and therefore also V_{exch} and $\Delta P/P_0$) is incorporated within a single physicochemical parameter $\alpha D^{1/2}$.

b. Bubble size spectra. In steady state or in a time-averaged sense, the rate at which intermediate and large bubbles are produced should equal the rate at which they reemerge at the surface. Accordingly, the bubble source spectrum can be estimated according to

$$Q(r) = U(r)g(r) \tag{22}$$

where $g(r)$ is the average size distribution immediately below the sea surface, i.e. the number of bubbles per unit volume of seawater with radii between r and $r + dr$.

Bubble size and depth distributions have been measured photographically in the open ocean by Kolovayev (1976) at depths of 1.5 to 8 m, by Johnson and Cooke (1979) at depths of 0.7 to 4 m, and by Walsh and Mulhearn (1987) at depths of 0.5 to 2.0 m. The studies show that the bubble size distribution, although highly variable, is reasonably well represented by a power law r^{-s} with s lying somewhere between 3.5 and 5 for bubbles with sizes between 0.01 and 0.035 cm in radius. No bubbles larger than 0.035 cm are reported in any of these studies. Also, none of these studies examined bubbles at depths shallower than 50 cm, so we would need to know how to extrapolate their results to the surface before making use of their results.

Even if it could be assumed that the size distribution is independent of depth, which is questionable, another serious difficulty is encountered in applying the oceanic bubble observations to calculate gas fluxes. The problem is how to extrapolate Eq. (22) to bubbles larger than 0.035 cm in radius. One common approach (e.g. Memery and Merlivat (1985a, b), Woolf and Thorpe (1991)) is to extrapolate the fixed power law for $g(r)$ to larger bubble radii. This approach is questionable, however, because the steep decline in observed bubble spectra from 0.01 to 0.035 cm is partly attributable to the rapid increase in rise velocity over this range. Beyond 0.035 cm the rise velocity increases only modestly (see Fig. 1) so $g(r)$ might be expected to decrease less rapidly beyond 0.035 cm. Thus this approach may significantly underestimate the importance of larger bubbles.

Perhaps a more reasonable approach to extrapolating the data to larger bubbles is to assume a fixed power-law for $Q(r)$, rather than a fixed power-law for $g(r)$. If we take $Q(r) \propto r^{-2}$ on the basis of $U(r) \propto r^2$ and $g(r) \propto r^{-4}$, as is appropriate for small bubbles, and extrapolate this relation to larger bubbles, we find that the integrals for exchange parameters (Eqs. (15) and (16)) actually diverge in the large radius limit. This divergence is obviously unphysical, and results from extrapolating the power law beyond its range of validity. Nevertheless, this divergence underscores the inadequacy of the existing photographic observations of bubble populations as a basis for calculating gas exchange rates.

Although very little information is available on the abundances of bubbles larger than 0.035 cm in the open ocean, some insight is provided by laboratory simulations. Broecker and Siems (1984) report observations of bubbles in the range from 0.01 to 0.1 cm in radius in a wind/wave tunnel at a depth of 20 cm. They obtain an average distribution characterized by $s = 3 \pm 0.4$ over this size range. Baldy (1988), reports observations of bubbles in the range 0.03 to 0.15 cm in radius in a wind/wave tunnel at depths between 5 and 25 cm. Baldy's study is particularly interesting because it indicates that there is a significant shift in the spectrum of bubbles which occurs at a depth of approximately one half the critical wave height. Below the transition zone, the distribution is characterized by an exponent of approximately $s = 3.5$, while above this depth the distribution is characterized by $s = 2.5$. Above the transition zone, the bubbles are grouped in clusters which correlate with the passage of

individual waves, while below the transition zone the bubbles are more uniformly dispersed. Baldy has termed the upper zone the "generation zone," and the lower the "dispersion zone." Baldy's work raises the possibility that the oceanic bubble measurements, discussed above, might have recorded bubble populations in the dispersion zone alone and thereby have "missed" most of the large bubbles.

Although these two laboratory simulations extend our understanding of bubbles to the size range of 0.15 cm, they provide no information on the production of bubbles larger than 0.15 cm in radius. Furthermore, the integrals (Eq. (15) and (16)) still diverge in the large-radius limit if the spectra observed in these studies are extrapolated beyond 0.15 cm radius. It is evident, therefore, that additional information on the largest bubbles is needed before we can make reliable estimates of bubble-induced gas exchange parameters.

One study which detected bubbles of arbitrarily large size is that of Monahan and Zeitlow (1969) who observed the size-distribution of bubbles on the water surface following a breaking wave in a simulation tank experiment. Assuming bubbles appeared on the surface in their experiment with the same spectrum as which they were produced, we can directly interpret their data in terms of bubble production rates. Their data suggest that the bubble production rate scales as $Q(r) \propto r^{-2.5}$ from radii of 0.04 to 0.4 cm. Above 0.4 cm the bubble populations decrease precipitously.

Another study which measured bubbles of arbitrarily large sizes is that of Cipriano and Blanchard (1981), who observed the spectrum of bubbles produced in a laboratory experiment aimed at simulating a plunging breaker. They report the source spectrum directly, so we do not need to calculate the spectrum as per Eq. (22). Both the Cipriano and Blanchard (1982) and the Monahan and Zeitlow (1969) spectra are shown in Figure 2. The two spectra are similar in shape over radii from 0.04 to 0.2 cm, but the Monahan and Zeitlow spectrum includes larger contributions from bubbles outside this range. These differences may reflect true differences in spectra produced for different types of breaking waves, e.g. spilling versus plunging breakers, or they may represent an artifact in one of the experiments.

In calculations below, the Monahan and Zeitlow spectrum and the Cipriano and Blanchard spectrum are employed alternately, as these spectra appear to represent the best available information on the production rates of bubbles larger than 0.035 cm. Direct oceanic observations of the relative abundances and production rates of large bubbles are clearly needed to resolve uncertainties in the bubble source distribution. It should be noted that the bubble source distribution may depend on a variety of conditions including, for example, sea state, surface tension, viscoscity, ionic strength etc. (see e.g. Shatkay and Ronen, 1992).

c. Total air entrainment rates. So far we have specified the shape of the bubble spectrum, but not its absolute magnitude. The magnitude is fixed by specifying the

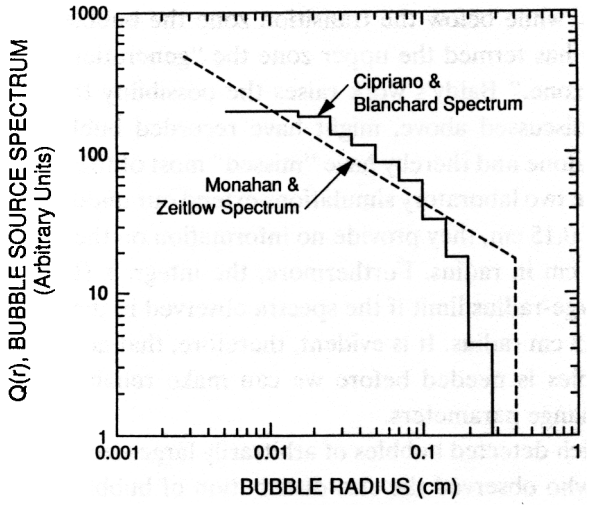

Figure 2. Bubble source spectra (i.e. number of bubbles produced per unit area, per unit time, per unit radius interval) observed by Cipriano and Blanchard (1981) (solid line) and inferred from the study of Monahan and Zeitlow (1969) (dashed line).

total air entrainment velocity, given by

$$V_{tot} = \int \frac{4\pi}{3} r^3 Q(r)\, dr$$

where V_{tot} has units of velocity. V_{tot} can be estimated based on the fraction of the sea surface covered with whitecaps and based on the rate at which air is vented through the surface of whitecaps.

Monahan and Lu (1990) distinguish between two types of white caps: Stage A whitecaps which are "the aerated spilling wave crest or active whitecaps," and Stage B white caps which are "the mature white cap or foam patch into which each Stage A white cap immediately decays into." The Stage A whitecaps are associated with concentrated transient bubble plumes while Stage B whitecaps are associated with more widely dispersed plumes (Monahan and Lu, 1990).

Recent laboratory measurements (Lamarre and Melville, 1991) indicate that the volume fraction of air, or void fraction, contained in concentrated transient bubble plumes decays from an initial value of around 10 or 20% to around 1% as the bubble plume ages and dissipates. Assuming that void fractions from 1 to 10% are typical of the concentrated plumes, it follows that the air evasion velocity (i.e., the volume of air per unit area per unit time escaping through the surface) of Stage A whitecaps should lie in the range of 0.3 to 3 cm sec^{-1}). This estimate assumes that the concentrated bubble plumes rise to the surface at approximately 30 cm sec^{-1}, the terminal rise velocity for large bubbles (Levich, 1962).

An alternate estimate of the air vented through active whitecaps can be derived from the laboratory simulations of Cipriano and Blanchard (1981). Their "model" whitecap had an effective diameter of "no greater than 16 cm" and was associated with an air flux of 125 ± 17 $cm^3\ sec^{-1}$. Together, these yield an air evasion velocity for their model whitecap of no less than 0.62 cm sec^{-1}, which lies within the range of 0.3 to 3 cm sec^{-1} estimated above.

Void fractions of Stage B whitecaps are evidently much smaller, typically around $2 \cdot 10^{-4}$ (Monahan and Lu, 1990; Monahan, 1991). With 30 cm sec^{-1} as an upper bound to the rise velocity of these plumes, the air evasion velocity of a typical Stage B whitecap is estimated to be no larger than $6 \cdot 10^{-3}$ cm sec^{-1}. Generally, around ten times as much of the sea surface is covered with Stage B whitecaps as Stage A whitecaps (Monahan and Torgersen, 1990). On this basis it can be seen that at least 98% of the air entrained in a breaking wave is vented through the surface of the associated Stage A whitecap while less than 2% is vented through the surface of the subsequent Stage B whitecap.

It appears, therefore, that the total air entrainment velocity can be estimated based on the relation

$$V_{tot} = V_A W_A \tag{24}$$

where V_A is the evasion velocity of air vented through the top of a Stage A whitecap and W_A is the fraction of the sea surface covered with Stage A whitecaps. According to Monahan and Torgensen (1990), the fraction of the sea surface covered with Stage A whitecaps at 20°C can be represented approximately as a function of windspeed according to

$$W_A = 1.85 \cdot 10^{-6} (U_{10} - 2.27)^3 \tag{25}$$

where U_{10} is the 10-meter wind speed in m sec^{-1}. At windspeeds below 2.27 m sec^{-1}, the whitecap coverage is taken as zero. With this formula the global average Stage A whitecap coverage of $\approx 0.1\%$ (Erickson *et al.*, 1986; Monahan and Torgersen, 1990) is obtained at a windspeed of approximately 10 m sec^{-1}.

In calculations below, total air-entrainment velocities will be calculated from (24) and (25) and V_A = 1.0 cm sec^{-1} will be adopted as a "best guess" case. This case would correspond to a global-average total air entrainment velocity of 0.001 cm sec^{-1}. Additional sensitivity studies will also be carried out using V_A = 0.3 and 3.0 cm sec^{-1}.

d. Characteristic bubble depths. Experimental observations of bubble populations in the open ocean suggest that the characteristic (*e*-folding) depth of small bubbles is approximately 1 meter with only a weak dependence on wind-speed or sea state (Wu, 1981; Thorpe, 1982; Crawford and Farmer, 1987). These observations, however, focused only on the diffuse plumes of bubbles smaller than 0.035 cm radius, which, as

shown above, comprise only a small fraction of the total air entrainment, and as shown below, only contribute a small fraction to K_b^{out}.

Very little information is available on the vertical distribution of the intense bubble plumes associated with Stage A whitecaps. Laboratory measurements of Lamarre and Melville (1991) indicate that the depth of the intense bubble plumes may have a complicated dependence on the conditions which produce breaking waves. In general, the plumes have a characteristic depth that is of the order of one half the wave amplitude. A similar scaling with wave height can be inferred from the work of Baldy and Bourguel (1987). If such a scaling is valid, this implies that the characteristic depth of the bubble plumes could vary significantly depending on wave age and sea state.

On the other hand, there should be a close association between the depth of an intense bubble plume and the lifetime of the associated whitecap. Lifetimes of the order of 1 second should correspond to depths of the order of 30 cm. This follows from assuming the intense plumes rise to the surface at a velocity of around 30 cm sec^{-1}, the terminal rise velocity of large bubbles. The observation that the lifetime of Stage A whitecaps rarely exceeds 1 second (Monahan and Lu, 1990) thus implies that the depth of stage A whitecaps rarely exceeds 30 cm, even in high seas.

More observations are needed to determine the sensitivity of bubble characteristic depth to sea state and bubble radius. Below, gas exchange parameters are calculated under three different assumptions for the characteristic depth: (1) a uniform characteristic depth of 25 cm ("best guess" case), (2) a uniform characteristic depth of 100 cm, and (3) a characteristic depth of 100 cm for bubbles smaller than 0.05 cm radius, and of 25 cm for bubble larger than 0.05 cm radius.

5. Calculations of exchange parameters

a. Calculations for bubbles of a single size. It is instructive to begin by computing exchange parameters for bubbles of a single size. The critical dimensionless parameter dictating the nature of the exchange process is ratio H_{eq}/z_0 which determines the degree to which the bubbles equilibrate with the water. The gas will fully equilibrate if $H_{eq}/z_0 \ll 1$ and will not equilibrate if $H_{eq}/z_0 \gg 1$. The equilibration distance H_{eq} is an increasing function of radius and a decreasing function of $\alpha D^{1/2}$ as seen in Figure 3.

For bubbles of a single size Eqs. (15) and (16) can be simplified to

$$V_{exch} = V_{tot}E(r) \tag{26}$$

and

$$\frac{\Delta P}{P_0} = \frac{F(r)}{E(r)}.$$

Figure 4a shows the results for the exchange efficiency V_{exch}/V_{tot} for bubbles with

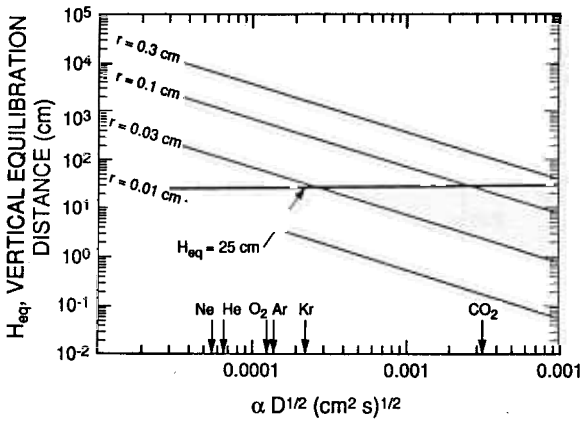

Figure 3. Vertical equilibration distance H_{eq} versus bubble radius for bubble radii in the range 0.01 to 0.3 cm computed using Eqs. (20) and (21). If a characteristic bubble depth of 25 cm is assumed, then the horizontal line at $H_{eq} = 25$ cm indicates the conditions (bubble radius and physicochemical constant $\alpha D^{1/2}$) where an initial saturation anomaly in bubbles of a given size is reduced on average by 50%. Above the line, the initial saturation anomalies are reduced on average by less than 50%, below the line they are reduced by more than 50%.

radii of 0.01, 0.3, 0.1, and 0.3 cm assuming, in all cases, a characteristic bubble depth of $z_0 = 25$ cm. For the smaller bubbles, we see that V_{exch}/V_{tot} approaches the limit of 1.0 corresponding to full equilibration, and thus, from Eq. (9), that the transfer velocity K_b^{out} for these small bubbles will scale as α^{-1} and is independent of diffusivity. For the large bubbles V_{exch}/V_{tot} tends to increase in proportion to $\alpha D^{1/2}$, which, from Eq. (9) implies that K_b^{out} for large bubbles scales as $D^{1/2}$ and is independent of solubility. Since bubbles of intermediate sizes yield scaling laws which lie in between these two limits, it follows that K_b^{out} always decreases with solubility but not more rapidly than as α^{-1}, and K_b^{out} always increases with diffusivity but not more rapidly than as $D^{1/2}$. Importantly, these results also hold for an arbitrary spectrum of bubble sizes.

Figure 4b shows the dependence of the effective over-pressure $\Delta P/P_0$ on the physicochemical parameter $\alpha D^{1/2}$ for these same bubble sizes. In the slow equilibration limit (large r, small $\alpha D^{1/2}$) the effective overpressure equals z_0/H_0 which is simply the average overpressure experienced by the bubbles. In the rapid equilibration limit (small r, large $\alpha D^{1/2}$) the effective overpressure scales as $\Delta P/P_0 = H_{eq}/H_0$ which converges towards zero in this limit. Thus, in this rapid equilibration limit, the effective overpressure is independent of the characteristic depth z_0. Here the insensitivity to z_0 arises because the gas in the bubble always re-equilibrates near surface regardless of how deep the bubble is initially carried.

b. Calculations with full bubble spectra. We now turn to the calculation of exchange parameters using the full bubble spectra. In order to explore the sensitivity of the computed exchange parameters to model input parameters, eight separate calcula-

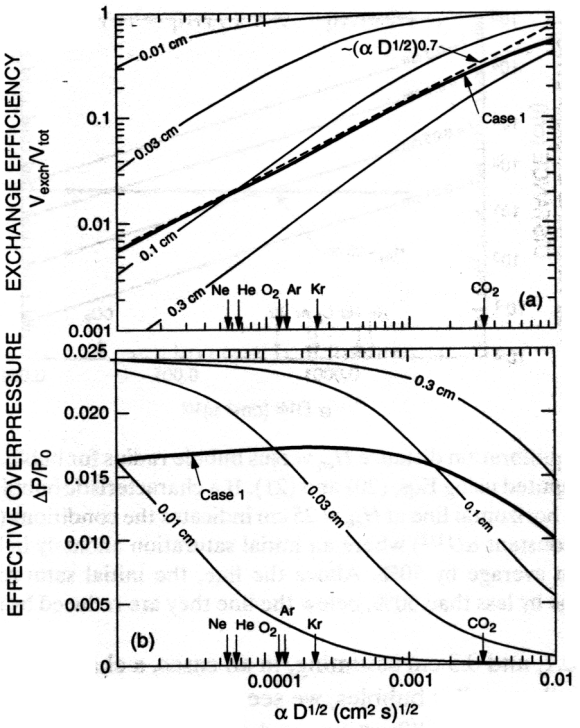

Figure 4. Exchange parameters V_{exch}/V_{tot} (a) and $\Delta P/P_0$ (b) versus physicochemical constant $\alpha D^{1/2}$ assuming the exchange is due to bubbles of a single size. Curves shown are for bubble sizes r = 0.01, 0.03, 0.1, and 0.3 cm. Also shown are exchange parameters computed for Case 1 using the bubble source spectrum inferred from study of Monahan and Zeitlow (1969) (see Fig. 2). All computations were performed assuming a characteristic bubble depth of 25 cm.

tions are carried out using different choices for the input parameters as summarized in Table 2.

The relative contribution of bubbles of different sizes to K_b^{out} is shown in Figure 5a for the "best guess" case (Case 1). In order to facilitate comparisons between different gases, the curves for different gases have been scaled by $D^{-1/2}$. This scaling is advantageous because $K_b^{out}D^{-1/2}$ would be the same for all gases if bubble-induced gas exchange had the same dependence on physicochemical properties as exchange through the sea surface (which is normally assumed to scale as $K_s \propto D^{1/2}$). It is seen that bubble-induced gas exchange is proportionally more important for gases with smaller values of the physicochemical constant $\alpha D^{1/2}$, e.g. bubbles are more important for He than O_2, and more important for O_2 than CO_2. It is also seen that smaller bubbles contribute to most of the differences between gases.

As mentioned above in Section 3, the model may overestimate the contribution of bubbles smaller than 0.03 cm because the model neglects the tendency of these smaller bubbles to disappear by dissolution, i.e. it neglects air injection. Even with

Table 2. Summary of input parameters for calculations.

Case	z_0	$k(r)$	V_A (cm sec^{-1})	$Q(r)$	Comments
1	25 cm	Eq. 21	1.0	$\propto r^{0.5}$; cutoff @ 0.4 cm	"Best guess" case
		Eq. 21	0.3	$\propto r^{0.5}$; cutoff @ 0.4 cm	Test sensitivity to V_A
3	25 cm	Eq. 21	3.0	$\propto r^{0.5}$; cutoff @ 0.4 cm	
4	25 cm	Eq. 21	1.0	$\propto r^{0.5}$; cutoff @ 0.6 cm	Test sensitivity to bubble spectrum
5	25 cm	Eq. 21	1.0	per Cipriano and Blanchard (1981)	
6	100 cm	Eq. 21	1.0	$\propto r^{0.5}$; cutoff @ 0.4 cm	Test sensitivity to bubble depth
7	See below*	Eq. 21	1.0	$\propto r^{0.5}$; cutoff @ 0.4 cm	
8	25 cm	4×	1.0	$\propto r^{0.5}$; cutoff @ 0.4 cm	Test sensitivity to $k(r)$

*Z_o = 25 cm for $r > 0.05$ cm and Z_o = 100 cm for $r \leq 0.05$ cm.

this overestimation, however, it is found for Case 1 that bubbles smaller than 0.03 cm contribute to only 29% of K_b^{out} for He, 19% for O_2, and 4% for CO_2. Thus the error in K_b^{out} caused by neglecting the disappearance of small bubbles is not likely to be very significant.

The contribution of bubbles of different sizes to $(\Delta P/P_0)\ K_b^{out}$, i.e. to the "exchange" contribution to $K_b^{in} - K_b^{out}$, is shown in Figure 5b for Case 1. Again curves have been scaled by $D^{-1/2}$. The dominance of large bubbles is again clearly indicated: bubbles smaller than 0.03 cm in radius contribute to only 10% of $(\Delta P/P_0)K_b^{out}$ for He, 4% for O_2, and 0.1% for CO_2. Importantly, this shows that the "exchange" contribution to $K_b^{in} - K_b^{out}$ is produced by bubbles of a completely different size range than the air injection processes, which is dominated by bubbles smaller than 0.03 cm in radius (Jähne *et al.*, 1984; Memery and Merlivat, 1985b).

Results for the exchange efficiency V_{exch}/V_{tot} and effective overpressure $\Delta P/P_0$ are shown above in Figure 4a and 4b for Case 1. The exchange efficiency is seen to scale nearly as a simple power law $((\alpha D^{1/2})^{0.7})$ over the full range from He to CO_2, although, as shown below, this result depends somewhat on the bubble source and depth spectrum. The effective overpressure varies from 0.018 to 0.013 compared to a value of 0.025 which might be expected based on the characteristic bubble depth of 25 cm.

The transfer velocity K_b^{out} for He, O_2, and CO_2 computed for Case 1 is plotted as a function of wind speed in Figures 6a to 6c. Also shown are results for Cases 2 and 3

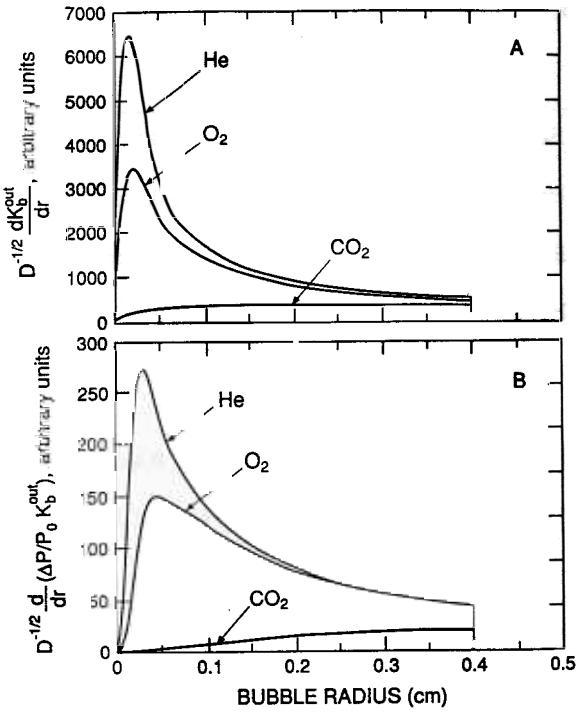

Figure 5. (a) The contribution of bubbles of different sizes to $K_b^{out}/D^{1/2}$ (i.e. the area under these curves yields $K_b^{out}/D^{1/2}$) for He, O_2 and CO_2. The curves were generated by dividing the integrand in Eq. (15) by $\alpha D^{1/2}$ (see also Eq. 9). The curves are arbitrary up to a multiplicative constant. This arbitrary constant effects equally the curves for all gases, so it doesn't effect comparison between different gases. (b) The contribution of bubbles of different sizes to $(\Delta P/P_0)\ K_b^{out}/D^{1/2}$ for He, O_2 , and CO_2. The curves were generated by dividing the integrand in Eq. 16 by $\alpha D^{1/2}$. The calculations here and throughout this paper use diffusivity data for CO_2 and He from Jähne *et al.* (1987a) for O_2 from Wise and Houghton (1966) and solubility data for He from Weiss (1971), for O_2 from Weiss (1970), and for CO_2 from Weiss (1974), all at 20°C.

which correspond to selecting different values for V_A, the air evasion velocity for type A whitecaps. The calculations assume z_0 = 25 cm at all windspeeds, thus neglecting any possible dependence of z_0 on windspeed. Because K_b^{out} is proportional to V_A, the factor of 10 range allowed for V_A corresponds to a factor of 10 range in K_b^{out}. Case 2, which assumes V_A = 0.3 cm sec^{-1}, yields a bubble-induced tranfer velocity which is only a small fraction of the total transfer velocity, assuming this rate is given by the Liss and Merlivat (1986) formula. Case 3, which assumes V_A = 3.0 cm sec^{-1}, yields a bubble-induced transfer velocity at 10 m sec^{-1} which amounts to 65%, 50% and 25% of the Liss and Merlivat velocity for He, O_2, and CO_2, respectively.

The exchange component of the steady-state supersaturation $f_0^{(exch)}$ for He, O_2, and CO_2 for the Cases 1, 2 and 3 is shown in Figures 7a–c. These calculations are based on Eq. (13) with the assumption that K_s is described by the Liss and Merlivat

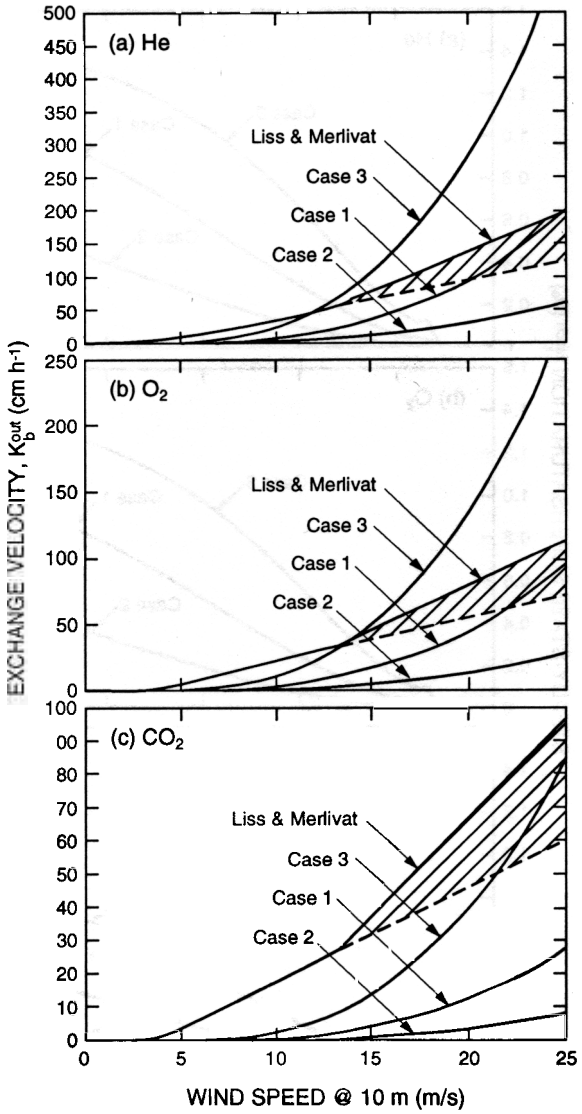

Figure 6. Outward exchange constant K_b^{out} versus windspeed computed for Cases 1, 2, and 3 (see Table 1) for He (a), O_2 (b), and CO_2 (c). Also shown is the exchange coefficient computed using the Liss and Merlivat relation. The hatched area below the Liss and Merlivat curve indicates the degree of enhancement assumed in the breaking wave regime by Liss and Merlivat.

formula for windspeeds below 13 m sec^{-1}. Above 13 m sec^{-1}, K_s is computed by linearly extrapolating the Liss and Merlivat formula for windspeeds between 3.6 and 13 m sec^{-1} to higher windspeeds. This normalization is reasonable because Liss and Merlivat incorporate a slope change at 13 m sec^{-1} in order to account for enhanced

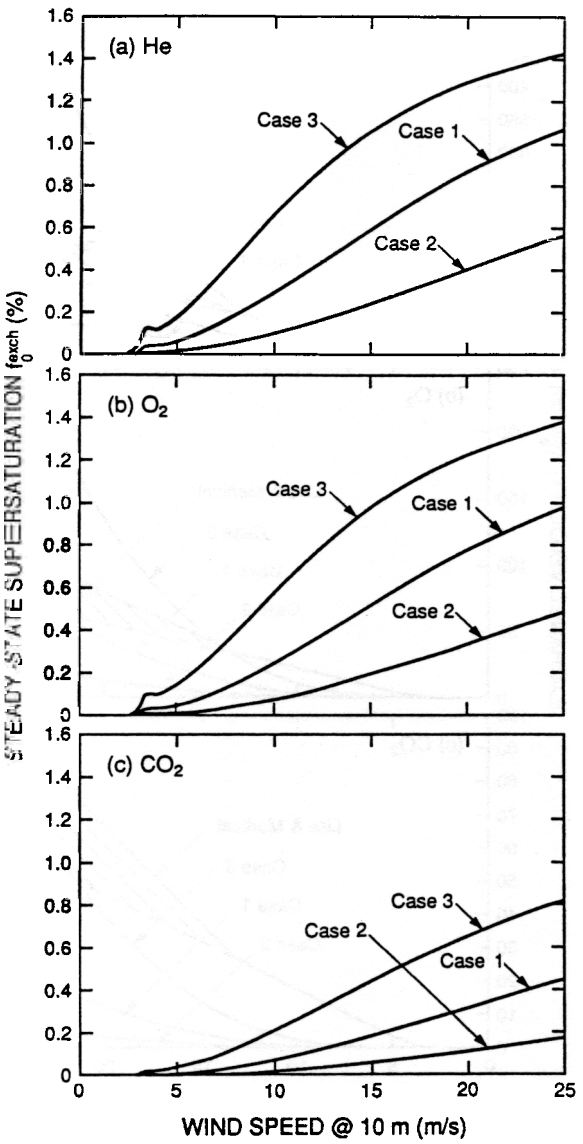

Figure 7. The "exchange" component of the steady-state supersaturation f_0^{exch} for Cases, 1, 2, and 3 (see Table 1) for He (A), O_2 (B), and CO_2 (C). The calculations assumes that the surface exchange coefficient K_s is given by the Liss and Merlivat (1986) relation (see text).

exchange due to wave breaking. At low wind speeds, the factor of 10 range allowed for V_A also corresponds to a factor of 10 range in $f_0^{(exch)}$. Here the steady-state supersaturation is approximately given by $(\Delta P/P_0)K_b^{out}/K_s$ which increases with windspeed roughly as U_{10}^2 (since $K_b^{out} \propto U_{10}^3$ and $K_s \propto U_{10}$). At high windspeeds, where

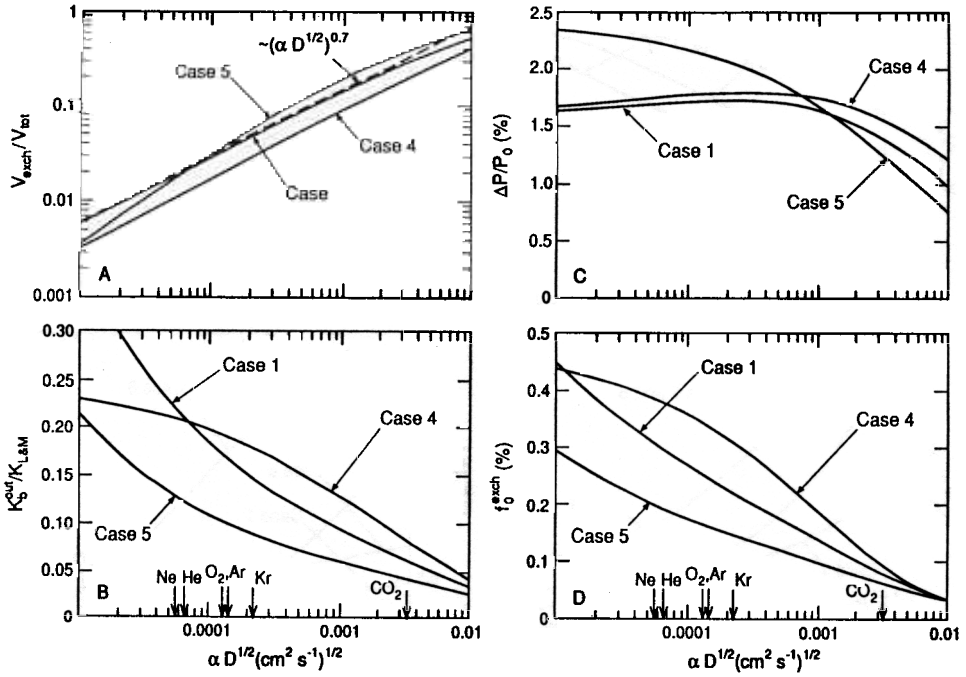

Figure 8. (a) The exchange efficiency V_{exch}/V_{tot} (b), ratio of outward exchange coefficient to the Liss and Merlivat exchange coefficient $K_b^{out}/K_{L\&M}$ (c), effective overpressure $\Delta P/P_0$ (d), and exchange component of the steady-state supersaturation $f_0^{(exch)}$, all at a wind speed of 10 m sec^{-1} versus $\alpha D^{1/2}$. Cases 1, 4, and 5 (see Table 2) explore the sensitivity of the exchange parameters to different bubble source spectra assuming a fixed total air entrainment rate.

$K_b^{out} \gg K_s$, the steady-state supersaturation approaches the maximum limit of $\Delta P/P_0$ which is independent of windspeed. If we adopt the results for Case 3, which assumes the highest possible total air entrainment velocity, the steady-state supersaturations at a windspeed of 10 m sec^{-1} amount to 0.7%, 0.6% and 0.2% for He, O_2, and CO_2 respectively. The other cases yield smaller steady-state supersaturations.

Cases 4 and 5 explore the sensitivity of the exchange parameters to the assumed bubble source spectra. Results for these cases, compared against Case 1, are shown in Figure 8a–d. Figure 8b shows the computed ratio $K_b^{out}/K_{L\&M}$ at 10 m sec^{-1}, where $K_{L\&M}$ is the transfer velocity computed from the Liss and Merlivat formula. Figure 8d shows the steady-state supersaturation computed at 10 m sec^{-1} assuming $K_s = K_{L\&M}$. The principal difference between the three bubble spectra is the relative abundance of bubbles larger than 0.2 cm radius, with Case 4 having the most and Case 5 having the fewest. In spite of these differences it is seen that the various exchange parameters differ by less than a factor of 2 when based on these different spectra. However it is clear from Figure 8a that if Case 5 is adopted then V_{exch}/V_{tot} can no

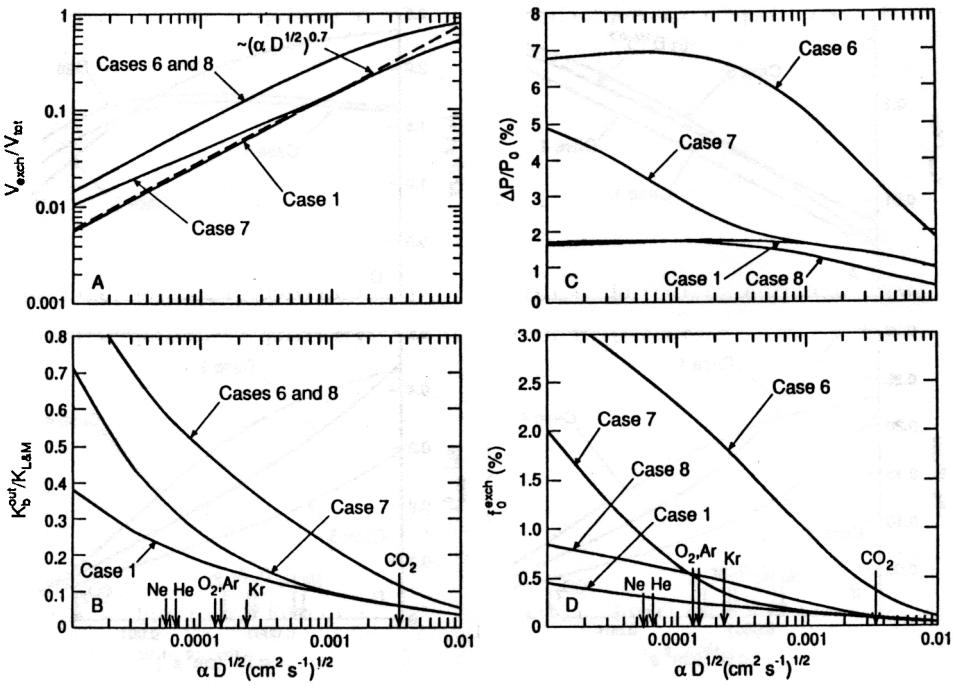

Figure 9. Same as Figure 8, for Cases 1, 6, 7, and 8 which explore the sensitivity of the exchange parameters to extending the $Q(r) \propto r^{-2.5}$ power law out to $r = 0.6$ cm (Case 6), a variable characteristic depth (Case 7), and more rapid gas exchange at the bubble-water interface (Case 8).

longer be well represented as a power-law in $\alpha D^{1/2}$ over the full range in $\alpha D^{1/2}$ from He to CO_2.

Results for Cases 6, 7, and 8, are shown in Figure 9a–d. In Case 6, the characteristic depth is increased to 100 cm for all bubble sizes, while in Case 7 the characteristic depth is increased to 100 cm only for bubbles smaller than 0.05 cm in radius. In Case 8 the transfer velocity $k(r)$ is increased uniformly by a factor of four for all bubble sizes. Case 8 effectively explores the sensitivity of the results to either $k(r)$ or $U(r)$ because both influence the calculations through the parameter H_{eq} alone.

In terms of the effects on V_{exch}/V_{tot} and K_b^{out} (Figs. 9a and 9b), it is seen that Cases 6 and 8 are indistinguishable. This is to be expected because both V_{exch}/V_{tot} and K_b^{out} depend only on the ratio $H_{eq}/z_0 \propto k(r)^{-1} z_0^{-1}$ (see Eq. 19) so that a fourfold increase in z_0 is equivalent to a fourfold increase in $k(r)$. Comparing Cases 6 and 8 with Case 1, we see that the fourfold increase in $k(r)$ or z_0 leads to a 3.2-fold increase in V_{exch}/V_{tot} and K_b^{out} at low $\alpha D^{1/2}$ and smaller increases at large $\alpha D^{1/2}$. These transfer velocities are not quite proportional to $k(r)$ and z_0 because, even at low $\alpha D^{1/2}$, a certain fraction of the exchange is carried by small bubbles which virtually equilibrate with the water, and the exchange contributed by these small bubbles is insensitive to $k(r)$ and z_0.

Increasing the depth of only the smaller bubbles, as in Case 7, has the effect of increasing the transfer velocity at small values of $\alpha D^{1/2}$ and leaving the transfer velocity virtually unchanged at large $\alpha D^{1/2}$. The transfer velocity for gases with large $\alpha D^{1/2}$ (e.g. CO_2) are relatively insensitive to the depth of the small bubbles because small bubbles contribute proportionally less of the exchange as $\alpha D^{1/2}$ is increased (see Fig. 5a).

The effective overpressure (Fig. 9c) is almost, but not quite, proportional to z_0 at low $\alpha D^{1/2}$ and less sensitive to z_0 at large $\alpha D^{1/2}$. An additional sensitivity test (not shown) indicated that as z_0 is increased beyond 100 cm a plateau in $\Delta P/P_0$ is eventually reached at a value of around 0.08 for soluble gases like CO_2. The plateau arises because a gas like CO_2 will always reequilibrate within about 80 cm of the surface (where the overpressure is ≈ 0.08) even if bubbles are initially carried much deeper than 80 cm. Increasing $k(r)$ has essentially no effect on the effective overpressure at low $\alpha D^{1/2}$ and actually decreases the effective overpressure at large $\alpha D^{1/2}$. This decrease arises because increasing $k(r)$ causes the gas in the bubble to reequilibrate closer to the surface where the overpressure is smaller.

The calculated steady-state supersaturation $f_0^{(\mathrm{exch})}$ is nearly, but not quite proportional to z_0^2 at low $\alpha D^{1/2}$ (Fig. 9d, Case 6). This follows because the steady-state supersaturation depends on the product of $K_b^{(\mathrm{out})}$ and $\Delta P/P_0$ both of which are nearly proportional to z_0 at low $\alpha D^{1/2}$, as discussed above. The steady-state supersaturation is somewhat less sensitive to z_0 at high $\alpha D^{1/2}$, although the sensitivity is still very significant. For example, the fourfold increase in z_0 from 25 to 100 cm increases $f_0^{(\mathrm{exch})}$ for CO_2 from 0.08% to 0.38% (Cases 1 and 8). Increasing the depth of only the smaller bubbles causes $f_0^{(\mathrm{exch})}$ to increase, especially at low $\alpha D^{1/2}$ (Fig. 9d, Case 7). This result is interesting because it suggests a possible mechanism for generating excess supersaturation of He relative to gases like O_2 without invoking the air injection process. The steady-state supersaturation f_0^{exch} is only very weakly sensitive to $k(r)$, with a four-fold increase in $k(r)$ leading to only a 40% increase in $f_0^{(\mathrm{exch})}$ at low $\alpha D^{1/2}$ and no change in $f_0^{(\mathrm{exch})}$ at high $\alpha D^{1/2}$ (Fig. 9d, Case 8). The insensitivity at high $\alpha D^{1/2}$ arises because changes in $\Delta P/P_0$ and $K_b^{(\mathrm{out})}$ tend to cancel each other out. These results show that the computed steady-state supersaturation for soluble gases like CO_2 is only weakly dependent on $k(r)$ and $U(r)$.

6. Discussion

An important conclusion of this study is that the bubble-induced gas exchange parameters $K_b^{(\mathrm{out})}$ and $\Delta P/P_0$ depend critically on the production rates of bubbles larger than 0.05 cm radius. This result would appear to shed some doubt on the recent modelling study of Wolfe and Thorpe (1991) in which the contribution of bubbles larger than 0.05 cm radius was assumed to be negligible. By neglecting larger bubbles, their study may underestimate substantially the role of bubbles in gas exchange and supersaturation, especially for soluble gases like CO_2. It should be

noted, however, that the relative production rates of large bubbles used in the present study are based solely on laboratory simulation experiments. Direct observations of the relative production rates of bubbles in the size range of 0.05 to 1 cm radius in active (Stage A) plumes are thus clearly needed to validate these calculations.

The Liss and Merlivat (1986) relation for the exchange coefficient incorporates a slope change at 13 m sec^{-1} which was included in order to account approximately for the enhanced gas exchange caused by breaking waves. It is encouraging that the model results lead to bubble-induced exchange rates which are of the right order of magnitude to account for this enhancement (see Fig. 6). This suggests that most if not all of the postulated enhancement at windspeeds above 13 m sec^{-1} can be accounted for on the basis of bubble entrainment.

The results imply that the total air-sea transfer velocity $K_{tot} = K_s + K_b^{out}$ at windspeeds above about 10 m sec^{-1} depends, not just on diffusivity, but also on the solubility of the gas. The Liss and Merlivat (1986) formulation, which neglects solubility effects, is thus incomplete at high windspeeds. The results for the "best guess" case suggest K_b^{out} should scale as $\alpha^{-0.3}D^{0.35}$ (corresponding to $V_{exch} \propto (\alpha D^{1/2})^{0.7}$). This result is somewhat uncertain, however, because of insufficient information on bubble size spectra and depth distributions. Nevertheless, the sensitivity studies performed above suggest that this scaling law should be valid to within about a factor of two over the full range of solubilities from He to CO_2.

According to the formulation presented here, the solubility dependence of bubble-induced gas exchange velocity is mathematically linked to the diffusivity dependence. The essential point is that αK_b^{out} is constrained to be a function of $\alpha D^{1/2}$ alone (see Table 1). This constraint is independent of the details of the model and depends only on the assumption that the exchange coefficient for an individual bubble, $k(r)$, scales as $D^{1/2}$. Recently, Asher *et al.* (1992) report results from a whitecap simulation tank which show an enhancement of gas exchange proportional to the fractional white-cap coverage. They found that the exchange velocity per unit white-cap coverage was proportional to $D^{0.3}$ but independent of solubility. Their result is not compatible with the above model constraint and therefore also not compatible with the sort of bubble-induced exchange process modelled here. The reason for the discrepancy is unknown at present.

An important limitation of the present study is that the absolute magnitude of K_b^{out} and thus the ratio K_b^{out}/K_{tot} is still highly uncertain. The "best guess" case suggests that K_b^{out} should equal 29% of the Liss and Merlivat rate for He, 25% for O_2, and 8% for CO_2 at windspeeds of 10 m sec^{-1}. These estimates are quite sensitive to a variety of model parameters which are not yet known with accuracy. The overall uncertainty in K_b^{out} is probably around a factor of five.

The present model results for K_b^{out} can be compared to the laboratory simulation experiment of Asher *et al.* (1992) which yielded a liquid-phase exchange velocity per

unit white-cap area of 3.8 cm sec^{-1} for O_2 at 20°C. By rearranging Eqs. (9) and (24), we can express the exchange velocity per unit white-cap area as

$$\frac{K_b^{\text{out}}}{W_A} = \left(\frac{V_A}{\alpha}\right)\left(\frac{V_{\text{exch}}}{V_{\text{tot}}}\right)$$

which yields K_b^{out}/W_A = 1.1 cm sec^{-1} for Case 1, the "best guess" case (V_A = 1 cm sec^{-1}, $V_{\text{exch}}/V_{\text{tot}}$ = .03, α = .027, appropriate for O_2 at 20°C). The Asher *et al.* results for O_2 are thus 3.5 times larger than the Case 1 results but agree quite well with the Case 3 results (V_A = 3 cm sec^{-1}).

The estimate of the exchange contribution to the steady-state supersaturation $f_0^{(\text{exch})}$ is also highly uncertain. The "best guess" case yields steady-state supersaturations at a windspeed of 10 m sec^{-1} of 0.29% for He, 0.25% for O_2, and 0.08% for CO_2 assuming that the surface exchange rate K_s is given by the Liss and Merlivat formula. The overall uncertainty in $f_0^{(\text{exch})}$ is estimated to be around a factor of 20 for insoluble gases like He and O_2 and around a factor of 10 for insoluble gases like CO_2 on the basis of uncertainties in bubble size and depth distributions, production rates, exchange rates, and surface exchange constant K_s.

It can be argued on independent grounds, however, that the estimates of $f_0^{(\text{exch})}$ for He and O_2 based on the "best guess" case are not likely to be too low by more than a factor of four. Recent inert gas measurements (Craig and Hayward, 1987 and Spitzer and Jenkins, 1989) suggest that the average bubble-induced supersaturations for He and Ar lie in the range of 1 to 2%. These observations constrain the sum of the "exchange" and the "injection" contributions, so that the "exchange" contribution alone would have to be even smaller than this. The "injection" contribution alone is generally believed to be around 1% (Craig and Hayward, 1987). The global average "exchange" contribution for He and O_2 (which has almost identical physicochemical properties as Ar), is thus not likely to be larger than about 1% or so, i.e. a factor of four larger than the estimate based on the "best guess" case at 10 m sec^{-1} (the windspeed at which global-mean conditions should be attained).

This upper bound to $f_0^{(\text{exch})}$ for insoluble gases also implies an upper limit to $f_0^{(\text{exch})}$ for soluble gases like CO_2. The sensitivity studies above show that any adjustment in model parameters which increased $f_0^{(\text{exch})}$ for CO_2 would increase $f_0^{(\text{exch})}$ for the insoluble gases by at least as large a factor. It appears, therefore, that the global mean steady-state supersaturation for CO_2 cannot be larger than 0.3% and most likely is around 0.08%.

The possibility that surface waters might be slightly supersaturated at steady-state (i.e. at zero net flux) was neglected by Tans *et al.* (1990) in their approach to computing oceanic CO_2 uptake (Robertson and Watson, 1992). Their estimated uptake would need to be increased 0.25 · 10^{15} g C yr^{-1} if we assume a steady-state supersaturation of 0.3%. Because 0.3% is an upper limit, the correction to the Tans *et al.* estimate is most likely smaller than this.

One parameter which contributes significantly to the overall uncertainty in the estimates is the total air-entrainment velocity V_{tot} since both K_b^{out} and $f_0^{(exch)}$ tend to scale linearly with V_{tot}. Direct measurements of entrainment rates are clearly needed, especially for large bubbles. The approach outlined above, based on observations of whitecap coverage and void fractions, seems promising.

Another parameter which significantly affects the calculated exchange rates is the characteristic depth z_0. Again, most needed are data for the depths of bubbles contained in the intense bubble plumes of active (Stage A) whitecaps. It would be valuable to know how sensitive plume depth is to wave height and other conditions of the sea surface and whether the same characteristic depth is appropriate for bubbles of all sizes.

The modelling effort presented above points out that bubble-induced gas exchange rates are quite sensitive to many factors which are difficult to determine. This high sensitivity suggests that it will be difficult to construct accurate estimates of bubble-induced gas exchange using a direct modelling approach, such as that attempted here. On the other hand, bubble-induced gas exchange has a number of observable consequences which would allow theories of bubble-induced gas exchange to be constrained.

One observable consequence is the supersaturation caused by bubbles. This supersaturation is closely related to the fraction of gas exchange contributed by bubbles. According to Eq. (13), if the exchange fraction of the steady-state supersaturation $f_0^{(exch)}$ and the effective overpressure $\Delta P/P_0$ could both be measured, the fraction of the total gas exchange contributed by bubbles could be directly calculated. Although direct measurement of $f_0^{(exch)}$ is difficult, it should be possible to determine $f_0^{(exch)}$ by extending the approach of Spitzer and Jenkins (1989) using simultaneous observations of the saturation anomalies of He, Ar, and perhaps other inert gases in combination with dynamic models for the mixed layer. Observations on a collection of gases are needed to distinguish the "exchange" fraction and "air-injection" fractions of the supersaturation and to distinguish bubble-induced supersaturation from saturation anomalies caused by heating and cooling of the surface waters. The effective overpressure is closely related to the depth of the bubble plumes so it should be possible to estimate it from observations of the depths of intense bubble plumes.

Another observable consequence of bubble exchange is that, at high windspeeds, the transfer velocity becomes dependent on solubility. Measurements of the difference in the transfer velocities for gases of different solubilities would thus constrain the bubble contribution. The dual tracer technique of Watson *et al.* (1991) would seem well suited to probing the dependence of exchange rates on solubility if appropriate tracers spanning a range of solubilities could be employed.

Additional constraints on the model would be provided by measuring gas concentrations in bubbles just before the bubbles reemerge at the surface. The estimated exchange coefficients depends on the quantity V_{exch}/V_{tot} which is simply a measure of

the fractional extent to which the gases in the bubbles equilibrate with the water. Thus a measurement of the gas concentrations in the bubble plumes would directly test the model predictions of V_{exch}/V_{tot}. Especially useful would be measurements of gases spanning a range of solubilities and diffusivities.

The modelling effort presented here is incomplete in several significant respects. First, the theory offers no means of estimating the air injection velocity V_{inj} so additional information will be needed to construct a theory which directly incorporates air injection. What is needed is a procedure for calculating V_{inj}/V_{tot} which, as stated earlier, will depend on the dissolved concentrations of the major gases. Second, the theory doesn't address the functional dependence of the bubble-induced gas exchange on temperature. The mechanisms of bubble production and dispersion depend on both viscosity and surface tension, both of which depend on temperature, so the true temperature dependence of bubble-induced gas exchange may be difficult to determine theoretically. Note that part of this temperature sensitivity could be readily incorporated using formulas for whitecap coverage which include temperature dependence (e.g. Monahan, 1991). Finally, the theory does not explicitly account for the role that bubbles might play in enhancing the surface exchange rate (K_s) by contributing to turbulence near the surface.

7. Summary

A formulation of bubble-induced gas exchange has been introduced which separates the bubble contribution into ingassing and outgassing velocities and which further separates the difference between ingassing and outgassing velocities into "air injection" and "exchange" components. One simplification which arises using this approach is that the outgassing velocity and the "exchange" component of the difference can safely be assumed to be independent of the dissolved concentrations of the major gases.

A simple model has been presented which allows the outgassing exchange velocity and the exchange contribution to the difference between ingassing and outgassing velocities to be estimated. The model incorporates data from laboratory simulation experiments on the bubble source spectra which suggest that a significant fraction of the bubble-induced gas exchange is carried by bubbles larger than 0.05 cm in radius. The model is used to conduct sensitivity studies of bubble-induced gas exchange to certain parameters. Critical parameters which have been identified include the relative production rates of bubbles larger than 0.05 cm in radius, the total air-entrainment velocity, the bubble depth distribution, and the exchange rates across individual bubbles. Uncertainty in the model parameters makes accurate estimates of bubble-induced gas exchange impossible at the present time.

Several conclusions appear independent of these uncertainties, however. The model suggests that bubbles formed by breaking waves probably contribute significantly to the total gas exchange at windspeeds above 10 m sec^{-1}. In this regime, the

total gas exchange rate depends both on diffusivity and on solubility, with smaller exchange rates for gases with higher solubilities. Drawing on constraints imposed by inert gas measurements, it is concluded that the global-mean steady-state supersaturation in CO_2 induced by bubbles is not larger than 0.3%, and is probably a factor of four or so smaller than this.

APPENDIX

The derivation of Eqs. (15) to (19) is presented here. This analysis accounts for changes with time in individual bubble radii caused by compression and decompression. These changes are important because, when a gas component is near to equilibrium with the water, the partial pressure changes induced by compression or decompression can be the dominant process driving net gas exchange. On the other hand, the analysis neglects the effect of radii changes on $k(r)$ and $U(r)$. In other words, the analysis assumes that these parameters are constant with time for an individual bubble, regardless of the changes in its radii.

Using the model of Memery and Merlivat (1985a), the gas flux carried by bubbles is given by $F_b = \int\int Z(r, z)N(r, z)\, drdz$ where Z is the bubble source, i.e. number of bubbles per unit radius which are initially submersed to depth z per unit time, and $N(r, z)$ is the total amount of gas transferred from an individual bubble into the water during its lifetime ($N(r, z)$ can be positive or negative). The bubble source function can be written $Z = U(r)\partial\Psi/\partial z$, where Ψ is the size-depth distribution of bubbles, i.e. the number of bubbles per unit radius per unit volume. Assuming the bubbles are distributed exponentially with depth, we have $\Psi = g(r)e^{z/z_0}$ where $g(r)$ is the bubble distribution at the surface, and where throughout this treatment z is defined to be zero at the surface and to decrease downward. Thus we have

$$F_b = \int_{-\infty}^{0}\int_{0}^{\infty} U(r)g(r)\frac{e^{z/z_0}}{z_0}N(r, z)\, drdz.$$

In order to calculate $N(r, z)$, we begin with the gas exchange caused by an individual bubble (Eq. (14)) which can be written

$$U\frac{dn}{dz} = kr^2S(P_l - P_b)$$

because $U = dz/dt$. Allowing for hydrostatic compression and decompression, the volume of the bubble will be given by $V = V_0P_0/(P_0 - \rho gz)$ where V_0 is the volume of the bubble at the surface, P_0 is the pressure at the surface, and ρ is the water density. It follows that the partial pressure in the bubble can be written

$$P_b = \frac{nRT}{V_0}\left(1 - \frac{\rho gz}{P_0}\right)$$

Combining Eqs. (30) and (31) yields,

$$U\frac{dn}{dz} = kr^2S\left[P_l - \frac{RT}{V_0}\left(1 - \frac{\rho gz}{P_0}\right)n\right] \tag{32}$$

We now define the following length scales

$$H_0 = \frac{P_0}{\rho g}; \qquad H_{eq} = \frac{V_0}{RT}\frac{U}{kr^2S} = \frac{4\pi}{3\alpha}\frac{rU}{k}$$

so that Eq. (32) can be written

$$\frac{dn}{dz} = \frac{1}{H_{eq}}\cdot\left[\frac{P_lV_0}{RT} - \left(1 - \frac{z}{H_0}\right)n\right]. \tag{34}$$

This has the form of a linear first-order equation with non-constant coefficients. We must seek a solution subject to the boundary condition that $n(r, z') = (P_gV_0)/(RT)$, where z' is the depth to which the bubble was initially submersed. The solution to Eq. (34) for the above boundary condition is

$$\begin{aligned} n(r,z) = {} & \frac{P_gV_0}{RT}e^{1/2(H_0/H_{eq})[(1-z_0/H_0)^2-(1-z'/H_0)^2]} \\ & + \frac{P_lV_0}{RT}\sqrt{\frac{2H_0}{H_{eq}}}e^{1/2\,H_0/H_{eq}(1-z/H_0)}\int_{\sqrt{H_0/2H_{eq}}(1-z/H_0)}^{\sqrt{H_0/2H_{eq}}(1-z'/H_0)} e^{-y^2}\,dy \end{aligned} \tag{35}$$

The total amount of gas transferred is given by $N(r, z') = n(r, z') - n(r, 0)$ which, from Eq. (35), yields

$$\begin{aligned} N(r,z') = {} & \frac{P_gV_0}{RT}(1 - e^{z'/H_{eq}(1-z'/2H_0)}) \\ & + \frac{P_lV_0}{RT}\sqrt{\frac{2H_0}{H_{eq}}}e^{1/2(H_0/H_{eq})}\int_{\sqrt{H_0/2H_{eq}}}^{\sqrt{H_0/2H_{eq}}(1-z'/H_0)} e^{-y^2}\,dy. \end{aligned} \tag{36}$$

We note that $N(r, z')$ is a linear function of P_g and P_l, and therefore that F_b in Eq. (29) is also a linear function of P_g and P_l.

Substituting Eq. (36) into Eq. (29) and matching coefficients of P_l and P_g with those in Eq. (4), we have

$$K_b = \left(\frac{4\pi}{3\alpha}\right)\int_0^\infty U(r)g(r)E(r)r^3\,dr$$

$$K_b^{in} - K_b^{out} = \left(\frac{4\pi}{3\alpha}\right)\int_0^\infty U(r)g(r)F(r)r^3\,dr \tag{38}$$

where

$$E(r) = \frac{1}{z_0}\sqrt{2\frac{H_0}{H_{eq}}}\, e^{1/2(H_0/H_{eq})} \int_{-\infty}^{0} e^{z'/z_0}\left[\int_{\sqrt{H_0/2H_{eq}}}^{\sqrt{H_0/2H_{eq}}(1-z'/H_0)} e^{-y^2}\, dy\right] dz' \tag{39}$$

$$F(r) = \frac{1}{z_0}\int_{-\infty}^{0} e^{z'/z_0}\, dz' - \frac{1}{z_0}\int_{-\infty}^{0} e^{z'/z_0}\, e^{z'/H_{eq}(1-z'/2H_{eq})}\, dz' - F(r). \tag{40}$$

The evaluation of the integral over z' in Eq. (39) can be carried out using integration by parts, and the integrations over z' in Eq. (40) can be carried out directly. After several further simplifications, this yields

$$E(r) = \sqrt{\frac{2H_0}{H_{eq}}}\, e^{H_0H_{eq}/2(1/z_0+1/H_{eq})} \int_{\sqrt{H_0H_{eq}/2}(1/z_0+1/H_{eq})}^{\infty} e^{-y^2}\, dy \tag{41}$$

and

$$F(r) = 1 - 2\frac{\sqrt{H_0H_{eq}}}{2}\left(\frac{1}{z_0}+\frac{1}{H_{eq}}\right) e^{H_0H_{eq}/2(1/z_0+1/H_{eq})^2} \int_{\sqrt{H_0H_{eq}/2}(1/H_0+1/H_{eq})}^{\infty} e^{-y^2}\, dy \tag{42}$$

which can be further simplified to yield

$$E = \sqrt{\frac{2H_0}{H_{eq}}}\, I(\Theta) \tag{43}$$

$$F = 1 - 2\Theta I(\Theta) \tag{44}$$

$$\Theta = \sqrt{\frac{H_0H_{eq}}{2}}\left(\frac{1}{z_0}+\frac{1}{H_{eq}}\right) \tag{45}$$

$$I(\Theta) = \frac{\sqrt{\pi}}{2}\, e^{\Theta^2}\, erfc\,(\Theta) \tag{46}$$

where

$$erfc\,(\Theta) = \frac{2}{\sqrt{\pi}}\int_{\Theta}^{\infty} e^{-y^2}\, dy \tag{47}$$

is the complementary error function.

Even further simplification of $E(r)$ and $F(r)$ is possible if we recognize that Θ has a lower bound of $\sqrt{H_0/2z_0} \gg 1$. This allows us to replace the error function with its

asymptotic limit for large Θ:

$$erfc\,(\Theta) = \frac{e^{-\Theta^2}}{\Theta\sqrt{\pi}}\left(1 - \frac{1}{2\Theta^2} + \quad\right) \tag{48}$$

(Dwight, 1961) which yields

$$E(r) = \frac{z_0}{z_0 + H_{eq}} \tag{49}$$

$$F(r) = \frac{H_{eq}}{H_0}\frac{z_0^2}{(z_0 + H_{eq})^2} \tag{50}$$

Finally, we need to show that Eqs. (37) and Eqs. (38) correspond to Eqs. (15) and (16). This is easily done by using Eqs. (22), (9), (10), with $V_{inj} = 0$ in Eq. (10). We need to set V_{inj} to zero because our theory only relates to the bubble exchange processes caused by bubbles that are too large to dissolve significantly. That is, the theory relates only to the term $\Delta P/P_0\, V_{exch}/\alpha$.

Acknowledgments. The author was greatly assisted by useful discussions with Raymond Najjar, David Erickson, Greg Crawford, Berndt Jähne and Edward Monahan. Critical comments by two anonymous reviewers were also very helpful. This work was supported by NSF grant ATM-8720377. Additional support was provided by the Advanced Study Program at NCAR.

REFERENCES

Asher, W. E., P. J. Farley, R. Wanninkhof, E. C. Monahan and T. S. Bates. 1992. Laboratory and field experiments on the correlation of fractional area whitecap coverage with air/sea gas transport, *in* Precipitation Scavenging and Atmosphere-Surface Exchange, *2,* S. E. Schwartz and W. G. N. Slinn, eds., Hemisphere Publishing Corp., Washington D.C., 815–825.

Baldy, S. 1988. Bubbles in the close vicinity of breaking waves: statistical characteristics of the generation and dispersion mechanisms. J. Geophys. Res., *93,* 8239–8248.

Baldy, S. and M. Bourguel. 1987. Bubbles between the wave trough and wave crest levels. J. Geophys. Res., *92,* 2919–2929.

Broecker, H. Ch. and W. Siems. 1984. The role of bubbles for gas transfer from water to air at higher windspeeds. Experiments in the wind-wave facility in Hamburg, *in* Gas Transfer at Water Surfaces, W. Brutsaert and B. H. Jirka, eds., D. Reidel, Hingham, MA, 229–236.

Cipriano, R. J. and D. C. Blanchard. 1981. Bubble and aerosol spectra produced by a laboratory 'breaking wave.' J. Geophys. Res., *86,* 8085–8092.

Craig, H. and T. Hayward. 1987. Oxygen supersaturation in the ocean: biological versus physical contributions. Science, *235,* 199–235.

Craig, H. and R. F. Weiss. 1970. Dissolved gas saturation anomalies and excess helium in the ocean. Earth Planet. Sci. Letts., *10,* 289–296.

Crawford, G. B. and D. M. Farmer. 1987. On the spatial distribution of ocean bubbles. J. Geophys. Res., *92,* 8231–8243.

Dwight, H. B. 1961. Tables of Integrals and Other Mathematical Data. Macmillan, NY, 336 pp.

Erickson, D. J., J. T. Merril and R. A. Duce. 1986. Seasonal estimates of global oceanic whitecap coverage. J Geophys. Res., *91,* 12975–12977.

Fuchs, G., W. Roether and P. Schlosser. 1987. Excess ^{3}He in the ocean surface layer. J. Geophys. Res., *92,* 6559–6568.

IUPAC. 1979. Solubility Data Series, *2,* H. L. Clever, ed., Pergamon Press, NY, 357 pp.

Jähne, B., G. Heinz and W. Dietrich. 1987a. Measurements of the diffusion coefficients of sparingly soluble gases in water. J. Geophys. Res., *92,* 10767–10776.

Jähne, B., K. O. Münnich, R. Bösinger, A. Dutzi, W. Huber and P. Libner. 1987b. On the parameters influencing air-water gas exchange. J. Geophys. Res., *92,* 1937–1949.

Jähne, B., T. Wais and M. Barbaras. 1984. A new optical measuring device: A simple model for bubble contribution to gas exchange, *in* Gas Transfer at Water Surfaces, W. Brutsaert and B. H. Jirka, eds., D. Reidel, Hingham, MA, 237–246.

Johnson, B. D. and R. C. Cooke. 1979. Bubble populations and spectra in coastal waters: a photographic approach. J. Geophys. Res., *84,* 3761–3766.

Kolovayev, P. A. 1976. Investigation of the concentration and statistical size distribution of wind-produced bubbles in the near-surface ocean layer. Oceanology, *15,* 659–661.

Lamarre, E. and W. K. Melville. 1991. Air entrainment and dissipation in breaking waves. Nature, *351,* 469–472.

Ledwell, J. J. 1984. The variation of the gas transfer coefficient with molecular diffusivity, *in* Gas Transfer at Water Surfaces, W. Brutsaiert and B. H. Jirka, eds., D. Reidel, Hingham, MA, 293–302.

Levich, V. G. 1962. Physicochemical Hydrodynamics, Prentice-Hall, Englewood Cliffs, NJ, 700 pp.

Liss, P. S. and L. Merlivat. 1986. Air-sea gas exchange rates: introduciton and sythesis, *in* The Role of Air-Sea Exchange in Geochemical Cycling, P. Buat-Menard, ed., D. Reidel, 113–127.

Memery, L. and L. Merlivat. 1985a. Contribution of bubbles to gas transfer across an air-water interface, *in* Gas Transfer at Water Surfaces, W. Brutsaiert and B. H. Jirka, eds., D. Reidel, Hingham, MA, 247–253.

—— 1985b. Modelling of gas flux through bubbles at the air-water interface, Tellus, *37B,* 272–285.

Merlivat, L. and L. Memery. 1983. Gas exchange across an air-water interface: experimental results and modeling of bubble contribution to transfer. J. Geophys. Res., *88,* 707–724.

Monahan, E. C. 1993. Occurrence and evolution of acoustically relevant sub-surface bubble plumes and their associated, remotely monitorable, surface whitecaps, *in* Natural Physical Sources of Underwater Sound: Sea Surface Sound, B. R. Kerman, ed., Kluwer Academic Publishers, Dordrecht, 503–517.

Monahan, E. C. and M. Lu. 1990. Acoustically relevant bubble assemblages and their dependence on meteorlogical parameters. IEEE J. Oceanic Eng. *15,* 340–349.

Monahan, E. C. and I. O. Muircheartaigh. 1980. Optimal power-law description of oceanic whitecap coverage dependence on wind speed. J. Phys. Oceanogr., *10,* 2094–2099.

Monahan, E. C. and Torgersen. 1991. Enhancement of air-sea gas exchange by oceanic whitecapping, *in* Air-Water Mass Transfer, Second International Symposium, on Gas Transfer at Water Surfaces/ASCE, NY, 608–617.

Monahan, E. C. and C. R. Zeitlow. 1969. Laboratory comparisons of fresh-water and salt-water whitecapes. J. Geophys. Res., *74,* 6961–6966.

Moore, D. W. 1963. The boundary layer on a spherical gas bubble. J. Fluid Mech., *16,* 161–176.
Robertson, J. E. and A. J. Watson. 1992. Thermal skin effect of the surface ocean and its implications for CO_2 uptake. Nature, *358,* 738–740.
Shatkay, M. and D. Ronen. 1992. Bubble populations and gas exchange in hypersaline solutions: a preliminary study. J. Geophys. Res., *97,* 7361–7372.
Spitzer, W. S. 1989. Rates of Vertical Mixing, Gas Exchange, and New Production: Estimates from Seasonal Gas Cycles in the Upper Ocean near Bermuda. Woods Hole Oceanographic Institution, MS thesis, 161 pp.
Spitzer, W. S. and W. J. Jenkins. 1989. Rates of vertical mixing, gas exchange, and new production: estimates from seasonal gas cycles in the upper ocean near Bermuda. J. Mar. Res., *47,* 169–196.
Tans, P. P., I. Y. Fung and T. Takahashi. 1990. Observation constraints on the global atmospheric CO_2 budget. Science, *247,* 1431–1438.
Thorpe, S. A. 1982. On the role of clouds of bubbles formed by breaking waves in deep water and their role in air-sea gas transfer. Phil. Trans. Royal Soc. London, *A304,* 155–210.
—— 1984. The role of bubbles produced by breaking waves in super-saturating the near-surface ocean mixing layer with oxygen. Annales Geophysicae, *2, 1,* 53–56.
Walsh, A. L. and P. J. Mulhearn. 1987. Photographic measurements of bubble populations from breaking wind waves at sea. J. Geophys. Res., *92,* 14553–14565.
Wanninkhof, R. 1992. Relationship between wind speed and gas exchange over the ocean. J. Geophys. Res., *97,* 7373–7382.
Watson, A. J., R. C. Upstill-Goddard and P. S. Liss. 1991. Air-sea gas exchange in rough and stormy seas measured by a dual-tracer technique. Nature, *349,* 145–147.
Weiss, R. F. 1970. The solubility of nitrogen, oxygen, and argon in water and seawater. Deep-Sea Res., *17,* 721–735.
—— 1971. The effect of salinity on the solubility of argon in seawater. Deep-Sea Res., *18,* 225–230.
—— 1971. Solubility of helium and neon in water and seawater, J. Chem. Eng. Data, *16,* 235–241.
—— 1974. Carbon dioxide in water and seawater: the solubility of a non-ideal gas. Mar. Chem., *2,* 203–215.
Wise, D. L. and G. Houghton. 1966. The diffusion coefficients of ten slightly soluble gases in water at 10–60°C. Chem. Eng. Sci., *21,* 999–1010.
Woolf, D. K. and W. A. Thorpe. 1991. Bubbles and the air-sea exchange of gases in near-saturation conditions. J. Mar. Res., *49,* 435–466.
Wu, J. 1981. Bubble populations and spectra in near-surface ocean: summary and review of field measurements. J. Geophys. Res., *86,* 457–463.

Received: *1 September, 1992;* revised: *1 March, 1993.*